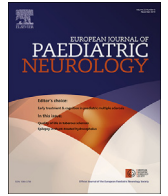




Contents lists available at ScienceDirect

European Journal of Paediatric Neurology



Structural brain anomalies in Cri-du-Chat syndrome: MRI findings in 14 patients and possible genotype-phenotype correlations

R. Villa ^{a,1}, V.G.C. Fergnani ^{a,1}, R. Silipigni ^b, S. Gueneri ^b, C. Cinnante ^c, A. Guala ^d, C. Danesino ^e, E. Scola ^c, G. Conte ^c, M. Fumagalli ^f, S. Gangi ^f, L. Colombo ^f, O. Picciolini ^g, P.F. Ajmone ^h, A. Accogli ^{i,j}, F. Madia ^j, E. Tassano ^j, M. Scala ^{i,j}, V. Capra ^j, M. Srouf ^{k,l}, L. Spaccini ^m, A. Righini ⁿ, D. Greco ^o, L. Castiglia ^o, C. Romano ^o, M.F. Bedeschi ^{a,*}

^a Medical Genetics Unit, Fondazione IRCCS Ca' Granda, Ospedale Maggiore Policlinico, Milan, Italy

^b Medical Genetics Laboratory, Fondazione IRCCS Ca' Granda Ospedale Maggiore Policlinico, Milan, Italy

^c Neuroradiology Unit, Fondazione IRCCS Ca' Granda Ospedale Maggiore Policlinico, Milan, Italy

^d Department of Pediatrics, Castelli Hospital, Verbania, Italy

^e Molecular Medicine Department, General Biology and Medical Genetics Unit, University of Pavia, Pavia, Italy

^f NICU, Department of Clinical Sciences and Community Health, Università degli Studi di Milano, Fondazione IRCCS Ca' Granda Ospedale Maggiore Policlinico, Milan, Italy

^g Pediatric Physical Medicine & Rehabilitation Unit, Fondazione IRCCS Ca' Granda Ospedale Maggiore Policlinico, Milan, Italy

^h Child and Adolescent Neuropsychiatric Service (UONPIA), Fondazione IRCCS Ca' Granda Ospedale Maggiore Policlinico, Milano, Italy

ⁱ DINOEMI, Università degli Studi di Genova, Italy

^j IRCCS Istituto Giannina Gaslini, Genoa, Italy

^k Department of Pediatrics, Division of Pediatric Neurology, McGill University, Montreal, Canada

^l McGill University Health Center (MUHC) Research Institute, Montreal, Canada

^m Clinical Genetics Unit, Department of Obstetrics and Gynecology, V. Buzzi Children's Hospital, University of Milan, Italy

ⁿ Department of Pediatric Radiology and Neuroradiology, V. Buzzi Children's Hospital, University of Milan, Italy

^o Oasi Research Institute, IRCCS, Troina, Italy

ARTICLE INFO

Article history:

Received 5 December 2019

Received in revised form

2 June 2020

Accepted 3 July 2020

Keywords:

Cri-du-chat syndrome

5p deletions

Brain MRI

Pontine hypoplasia

Neuroradiological phenotype

ABSTRACT

Introduction: Cri-du-Chat Syndrome (CdCS) is a genetic condition due to deletions showing different breakpoints encompassing a critical region on the short arm of chromosome 5, located between p15.2 and p15.3, first defined by Niebuhr in 1978. The classic phenotype includes a characteristic cry, peculiar facies, microcephaly, growth retardation, hypotonia, speech and psychomotor delay and intellectual disability. A wide spectrum of clinical manifestations can be attributed to differences in size and localization of the 5p deletion. Several critical regions related to some of the main features (such as cry, peculiar facies, developmental delay) have been identified. The aim of this study is to further define the genotype-phenotype correlations in CdCS with particular regards to the specific neuroradiological findings.

Patients and methods: Fourteen patients with 5p deletions have been included in the present study. Neuroimaging studies were conducted using brain Magnetic Resonance Imaging (MRI). Genetic testing was performed by means of comparative genomic hybridization (CGH) array at 130 kb resolution.

Results: MRI analyses showed that isolated pontine hypoplasia is the most common finding, followed by vermian hypoplasia, ventricular anomalies, abnormal basal angle, widening of cavum sellae, increased signal of white matter, corpus callosum anomalies, and anomalies of cortical development. Chromosomal microarray analysis identified deletions ranging in size from 11.6 to 33.8 Mb on the short arm of chromosome 5. Then, we took into consideration the overlapping and non-overlapping deleted regions. The

* Corresponding author.

E-mail addresses: roberta.villa1985@gmail.com (R. Villa), viola.fergnani@gmail.com (V.G.C. Fergnani), rosamaria.silipigni@policlinico.mi.it (R. Silipigni), silvana.gueneri@policlinico.mi.it (S. Gueneri), claudia.cinnante@policlinico.mi.it (C. Cinnante), andrea.guala@aslvc.it (A. Guala), cidi@unipv.it (C. Danesino), elisa.scola@policlinico.mi.it (E. Scola), giorgio.conte@policlinico.mi.it (G. Conte), monica.fumagalli@policlinico.mi.it (M. Fumagalli), silvana.gangi@policlinico.mi.it (S. Gangi), lorenzo.colombo@mangiagalli.it (L. Colombo), odoardo.picciolini@policlinico.mi.it (O. Picciolini), paola.ajmone@policlinico.mi.it (P.F. Ajmone), andreaaccogli@gaslini.org (A. Accogli), francescamadia@gaslini.org (F. Madia), elisatassano@gaslini.org (E. Tassano), marcelloscala87@gmail.com (M. Scala), vaelriacapra@gaslini.org (V. Capra), myriam.srouf@mcgill.ca (M. Srouf), luigina.spaccini@asst-fbf-sacco.it (L. Spaccini), andrea.righini@asst-fbf-sacco.it (A. Righini), dgreco@oasi.en.it (D. Greco), lcastiglia@oasi.en.it (L. Castiglia), cromano@oasi.en.it (C. Romano), mariafrancesca.bedeschi@policlinico.mi.it (M.F. Bedeschi).

¹ Roberta Villa and Viola Giulia Carlina Fergnani contributed equally to this work.

<https://doi.org/10.1016/j.ejpn.2020.07.002>

1090-3798/© 2020 European Paediatric Neurology Society. Published by Elsevier Ltd. All rights reserved.

Please cite this article as: R. Villa et al., Structural brain anomalies in Cri-du-Chat syndrome: MRI findings in 14 patients and possible genotype-phenotype correlations, European Journal of Paediatric Neurology, <https://doi.org/10.1016/j.ejpn.2020.07.002>

goal was to establish a correlation between the deleted segments and the neuroradiological features of our patients.

Conclusions: Performing MRI on all the patients in our cohort, allowed us to expand the neuroradiological phenotype in CdCS. Moreover, possible critical regions associated to characteristic MRI findings have been identified.

© 2020 European Paediatric Neurology Society. Published by Elsevier Ltd. All rights reserved.

1. Introduction

First described by Lejeune in 1963, Cri-du-Chat Syndrome (CdCS) (OMIM#123450) is a clinically recognizable contiguous gene syndrome ascribed to deletions in the short arm of chromosome 5 (5p). Its prevalence is estimated to 1:15.000–1:50.000 live births with a male-to-female ratio of 0.73 [1,2].

The disorder has a broad spectrum of manifestations; “classic” phenotype includes a characteristic high-pitched cat-like cry in infancy (hence the name of the syndrome), peculiar facies, microcephaly, growth retardation, hypotonia, speech and psychomotor delay and intellectual disability (ID) [1–5].

The clinical spectrum and the severity of the disease vary according to the size of the deletion and the position of the breakpoints. In general, a globally more severe psychomotor and intellectual phenotype is associated to large deletions, with proximal breakpoints localized in 5p14–5p13, whereas small deletions are associated to milder manifestations [3].

Structural brain malformations have been reported in CdCS patients, but their presence has not been studied systematically. Thus, detailed information regarding type and frequency of brain anomalies is still limited.

Case reports and the small case-series described by Tamraz *et al.*, suggest that the most typical neuroimaging findings are brainstem hypoplasia, most predominantly in the pons with or without cerebellar (or vermian) hypoplasia, and cerebellar white matter atrophy [6–19].

Other reported brain anomalies are thinning (or dysgenesis) of the corpus callosum, Dandy-Walker malformation, middle cerebellar peduncles hypoplasia, dilated ventricles (lateral, fourth) cerebellar interhemispheric cyst, arachnoid cyst, reduced myelination in anterior limbs of the internal capsule and large cisterna magna [6–8,10,15,17–19]. One recent autopsy study, in an 18 year-old girl with CdCS, revealed olfactory hypoplasia, focal hypoplasia of the brainstem, partial corpus callosum agenesis, cavum septum pellucidum, bilaterally polymicrogyria and multifocal neurodegenerative changes with intracytoplasmic inclusions in the hippocampus and cerebral neocortex [20].

Additionally, a flattened cranial base angle and malformation in the bony contours of the sella turcica and the clivus have been documented in a series of 23 patients with CdCS using lateral cephalometric radiograph [21].

In order to understand the pathogenic mechanisms of CdCS, it is important to exactly identify the deleted regions, the gene content and their potential contribution to the observed phenotype.

To date, the majority of the studies have focused on mapping the critical regions related to specific clinical features in CdCS, in particular the characteristic cry, the peculiar facial phenotype, microcephaly, language and development delay. Anyway, studies so far do not completely agree [22–30].

Molecular studies confirmed the role of these regions identifying, within them, the genes involved in different components of the classic phenotype.

To date, no genotype-phenotype correlation was proposed concerning neuroradiological features.

In the present study, we performed a systematic evaluation of brain MRI (Magnetic Resonance Imaging) studies of 14 unrelated patients with CdCS, analyzed by CMA (Chromosome Microarray Analysis), with the aims to further characterizing the spectrum of CNS (Central Nervous System) abnormalities found on brain MRI studies, and investigating genotype-phenotype correlation.

We hypothesize that a subset of genes in the commonly deleted region is dosage-sensitive and that the haploinsufficiency of one or more of these genes interferes with the normal development of the nervous system during embryogenesis. By comparing the size, localization and genetic content of the 5p deletions, we thus attempted to identify common overlapping regions between patients with the same neuroradiological phenotype and, within these regions, to highlight putative genes associated with brain malformations.

2. Patients and Methods

2.1. Patient cohort

A total of 14 patients (9 males and 5 females; age 0 month to 28 years), with cytogenetically confirmed diagnosis of CdCS and available brain MRI data, were enrolled through the collaborative effort of the contributing authors at the Medical Genetics Units, IRCCS “Ca’ Granda – Ospedale Maggiore Policlinico” Foundation of Milan.

Personal and family history were obtained for all patients. Referring physicians were asked to complete a standardized clinical checklist for their patients. The form included questions about family history, microcephaly [OFC (orbitofrontal cortex) <3rd percentile], hypotonia, developmental progress, behavioural problems, medical complications, minor facial anomalies (specifically with regard to Cri du Chat facial gestalt, including broad nasal bridge, epicanthal folds, micrognathia), other physical examination findings. All patients were clinically examined. Clinical evaluation for a dysmorphological assessment was performed by a medical geneticist according to international guidelines and was oriented to the detection of even minor anomalies and malformations. Some patients were regularly re-evaluated over several years and follow up data were recorded. Psychomotor development and intellectual disability assessments were based on age-target level tests and specialist evaluations.

Table 1 shows the age, the gender and a summary of the principal clinical information related this study cohort.

2.2. MRI study

Brain MRI was performed in all patients and neuroradiological data were revised by the Colleagues of the Neuroradiology Unit, IRCCS “Ca’ Granda – Ospedale Maggiore Policlinico” Foundation of Milan. Age of patients at MRI scan ranged from 5 days to 26 years (median value 5.5 months).

The MRI scans included T2 and T1 weighted sequences in all patients and FLAIR (Fluid-attenuated Inversion Recovery) images for patients older than 1 year. Images were acquired on axial, coronal and sagittal planes.

The MRI images assessment included the qualitative and quantitative evaluation of cerebral and skull anomalies and malformations. On the basis of available literature, specific neurologic abnormalities previously described, were intentionally sought. In particular, the presence of brainstem, pons, cerebellar vermis hypoplasia and optic nerve hypoplasia, of cortical, ventricles and corpus callosum malformations and anomalies of skull base angle and cavum sellae were assessed [31–34].

The skull base angle is the angle formed by the line extending across the anterior cranial fossa to the tip to the dorsum sellae and the line drawn along the posterior margin of the clivus. In children normal values are between 104–124° (means 113–115°) [35].

2.3. Cytogenetic and CMA studies

For each patient the diagnosis of CdCS was made on a clinical basis and confirmed by cytogenetic analysis (karyotype and FISH analysis).

Firstly, only a few patients (those more recently enrolled), were analyzed by CMA; then, new samples were collected, and CGH-array was performed on all patients.

Genomic DNA was isolated from peripheral blood sample using Gentra Puregene Blood Kit from Qiagen (Qiagen, Venlo, Netherlands), following the protocols provided by the manufacturers. A CGH-array analysis was performed using SurePrint G3 CGH 8×60 K Kit (Agilent Technologies, Santa Clara, CA, USA). Raw data were generated using Agilent Feature extraction and analyzed by Cytogenomics 4.0.3.12 software using ADM-2 algorithm (Agilent Technologies, Santa Clara, CA, USA). To improve the accuracy of the results, the Diploid Peak Centralization algorithm was applied. Aberrations were considered if at least three adjacent probes were involved and the Minimum Absolute Average Log Ratio (MAALR) was ± 0.25 . Copy number variations were not reported if they coincided with the published DNA variants listed in the Database of Genomic Variants (<http://projects.tcag.ca/variation/>). Genomic coordinates were defined according to the Human Genome build 37 (March 2009). Cytogenetic and FISH analysis of peripheral blood was carried out according to the standard laboratory procedure. Conventional karyotyping and FISH were performed according to the European General Guidelines and Quality Assurance for Cytogenetics [36] and genetic results were reported in accordance with the International System for Human Cytogenomic Nomenclature - ISCN [37].

All samples analyzed in this study were collected after adequate informed consent.

2.4. Ethical compliance

Informed consent was obtained from all parents/guardians before enrollment and after a full study description. The study was performed in accordance with the Declaration of Helsinki (1964) and was approved by the IRCCS “Ca’ Granda Ospedale Maggiore Policlinico” Foundation Scientific Board and, in agreement with Italian regulations, it does not require a specific ethical approval because it only uses anonymous data collected during routine patient care.

3. Results

3.1. Brain MRI findings

The neuroradiological findings observed at the brain MRI of the 14 patients are detailed in Table 2.

All enrolled patients showed malformation of the posterior fossa, formerly reported as a distinctive CdCS brain anomaly in literature.

Specifically, 7/14 cases displayed pontine and vermian hypoplasia and 6/14 cases showed isolated pontine hypoplasia. Isolated vermian hypoplasia was observed in 1/14 cases (Patient #6) who also had cerebellar vermis rotation (Fig. 1).

Corpus callosum abnormalities were observed in 11/14 patients. Specifically, MRI showed hypoplasia with dysmorphic or thin corpus callosum in 10 cases and a complete agenesis in 1 patient (Patient #9). Ten out of fourteen (10/14) cases displayed ventricular anomalies. Lateral ventricle enlargement was evident in 4 patients.

Cortical development abnormalities disorders were observed in 6/14 cases. Bilateral frontoparietal polymicrogyria was found in the imaging studies of 4/14 cases. Patient #7 exhibited right frontal lobe polymicrogyria. One case (Patient #11) had cortical nodular heterotopy.

Other findings included optical nerve hypoplasia in 3/14 cases, diffuse bilateral and symmetric increase of signal of white matter on T2 weighted images in 2/14 cases and bilateral hippocampus malrotation in (only) one case.

Basilar investigation showed widening of cavum sellae in 8/14 cases and basal angle anomalies in 4/14 cases.

Representative examples of brain MRI findings are provided in Fig. 2.

3.2. Cytogenetic and CMA results

All patients underwent CGH-array analysis to define size and localization of the deleted region on chromosome 5, as reported in Table 3. Eleven out of fourteen (11/14) patients showed terminal deletions, whereas 3 cases displayed interstitial deletions. The extension of the deleted region was variable from 11,6 to 33,8 Mb.

The Patient #12, showed a mosaic 14 Mb deletion in 5p. The mosaicism was confirmed by FISH using specific probe, with 60% of examined metaphases showing the deletion. The patient had a monozygotic twin found to have the same mosaic 5p deletion but in lower proportion (around 25% of examined cells). Chromosomal Mosaicism in CdCS is not uncommon compared to other structural aberrations. We speculate that the mosaicism of this case could result from a postzygotic unequal crossing-over event, occurred between repeated sequence on the short arm of chromosome 5, that caused a deleted 5p cell line. This might have happened early in development, before twinning.

None of the parents had clinical features of CdCS, suggesting that almost all cases were *de novo* events; FISH analysis was performed on all parents (except for Patient #11, #12 and #14, whose parents were not available for analysis) to investigate the presence of cryptic rearrangements.

The Patient #5, indeed, showed an unbalanced translocation determining a deletion on 5p and a duplication on 10q (18,3 Mb). Karyotype analysis of the parents revealed a balanced translocation between the short arm of chromosome 5 and the long arm of chromosome 10 in the father of the proband being the karyotype 46,XY,t(5;10)(p13.2;q25.3).

Moreover, in 3/14 cases the CMA analysis identified a second/third deletion or duplication involving another chromosome (Table 3). Patient #7 and #8 carried two small extra Copy Number Variations (CNVs) of likely benign and unknown clinical significance respectively. In Patient #11 a large terminal CNV of 5,2 Mb duplication on chromosome 15 has been identified, suggesting the presence of an unbalanced translocation between chromosome 5 and chromosome 15 of unknown origin. Indeed, parents' blood samples were not available for the cytogenetic analysis.

Table 1
Clinical features of the 14 patients with CdCS.

Patient	Sex	Age at diagnosis	Peculiar facies	Microcephaly*	Hypotonia	Developmental delay	Intellectual disability	Behavioural disorders	Heart anomalies	Ocular anomalies	Hearing impairment	Skeletal anomalies	Others
1	F	13 years	+	-	-	+	mild	anxiety disorder	-	myopia	bilateral moderate mixed deafness	kyphoscoliosis	menstrual irregularities, idiopathic hirsutism; lower limbs dysmetria
2	F	Birth	+	+	+	+	severe	-	IVD, PDA	-	-	-	GERD
3	M	8 months	+	-	+	+	moderate	hyperactivity, aggressivity, irritability	-	strabismus, hypermetropia, astigmatism	-	bilateral pes planus	-
4	F	Birth	+	+	+	+	moderate	aggressivity, irritability	IVD, PFO	astigmatism	-	bilateral pes planus-valgus	anorectal malformation
5	M	Birth	+	+	+	+	n.a.	-	pulmonary stenosis	papillae hypoplasia, retinal depigmentation	-	-	Hirschprung disease, GERD, aspecific EEG anomalies
6	M	14 months	+	+	+	+	severe	hyperkinesia, hyperactivity	prenatal atrial flutter	-	monolateral AABR fail	bilateral pes cavus-varus	hypertrophic pyloric stenosis
7	M	Birth	+	+	+	+	n.a.	-	pulmonary insufficiency	mild strabismus	-	-	cyanotic breath-holding spell
8	M	3 years	+	-	+	+	n.a.	-	-	strabismus	-	-	-
9	M	1 month	+	+	-	+	mild	aggressivity, irritability	IAD	hypermetropia, astigmatism	-	bilateral pes varus-adductus	-
10	F	3 months	+	+	+	+	severe	aggressivity, irritability	IVD	astigmatism, myopia	-	kyphoscoliosis	-
11	F	9 months	+	+	+	+	n.a.	-	-	strabismus, mild palpebral ptosis	-	-	laryngomalacia
12	M	2 months	+	+	+	+	n.a.	sleep disturbances	-	-	-	-	congenital hypothyroidism
13	M	4 months	+	+	+	+	n.a.	n.a.	mild tricuspid regurgitation	right side hyaloid remnant	monolateral AABR failed	bilateral metatarsus adductus	-
14	M	12 months	+	+	+	+	n.a.	n.a.	IVD, PFO	-	-	-	-

"+" = present; "-" = absent; "n.a." = not applicable, "IVD" = inter-ventricular defect; "PDA" = patent ductus arteriosus; "PFO" = patent foramen ovale; "IAD" = interatrial defect; "AABR" = automatic auditory brainstem response, "GERD" = gastroesophageal reflux disease. * Microcephaly: a OFC <3rd centile for age.

Table 2

Brain MRI imaging findings for each patient. "+" = present; "-" = absent.

Patient	Age at MRI	Pontine hypoplasia	Vermian hypoplasia	Ventricles anomalies	Basal angle anomalies	Widening of cavum sellae	Increased T2 signal from white matter	Corpus callosum anomalies	Cortical anomalies	Others
1	26 years	+	-	dysmorphic	>120°	dysmorphic	-	dysmorphic	-	
2	80 days	+	+	dysmorphic and widened	>120°	dysmorphic	-	dysmorphic	bilateral perisylvian polymicrogyria	optic nerves hypoplasia
3	5 days	+	-	normal	normal	dysmorphic	+	dysmorphic	-	optic nerves hypoplasia
4	53 days	+	+	dysmorphic	>120°	dysmorphic	+	dysmorphic	-	
5	61 days	+	+	dysmorphic	>120°	dysmorphic	-	dysmorphic	bilateral perisylvian polymicrogyria	hippocampus malrotation; optic nerves hypoplasia; reduction of white matter
6	14 months	-	+	dysmorphic	normal	normal	-	dysmorphic	-	cerebellar vermis rotation
7	5 days	+	+	dysmorphic	normal	normal	-	dysmorphic	right frontal lobe polymicrogyria	
8	19 months	+	-	normal	normal	dysmorphic	-	dysmorphic	-	
9	8 years	+	-	dysmorphic and widened	normal	normal	-	absent	bilateral perisylvian and parietal polymicrogyria	
10	4 years	+	+	dysmorphic and widened	normal	normal	-	dysmorphic	bilateral perisylvian polymicrogyria	
11	9 months	+	-	normal	normal	normal	-	normal	cortical nodular heterotopy	
12	30 days	+	+	normal	normal	dysmorphic	-	normal	-	
13	30 days	+	+	dysmorphic	normal	dysmorphic	-	normal	-	
14	12 months	+	-	dysmorphic and widened	normal	normal	-	dysmorphic	-	

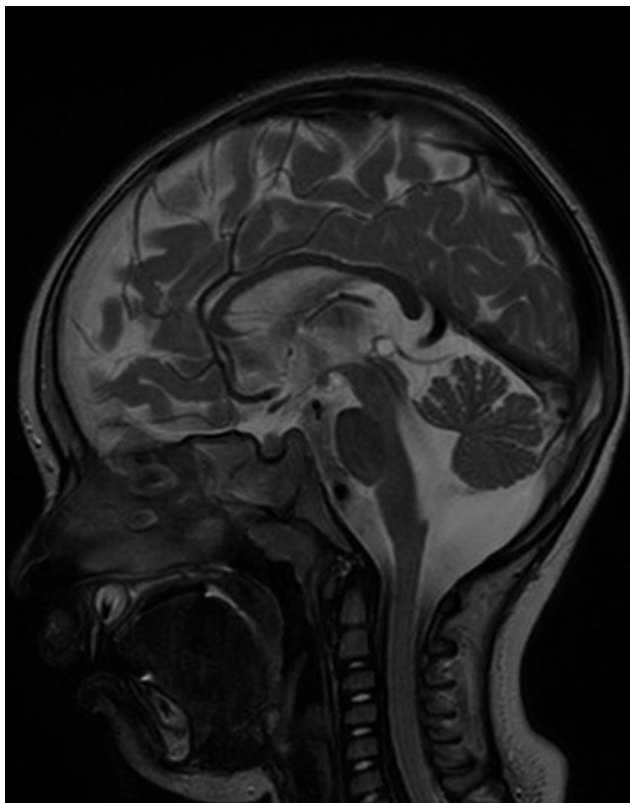


Fig. 1. Patient #6 brain MRI findings. Sagittal T2-weighted image showed normal brainstem morphology and small upward-rotated vermis, thus the IV ventricle appearing widened and opened inferiorly.

3.3. Genotype and neuroradiological findings correlation

As shown in Fig. 3, CMA analysis of our cohort allowed us to identify four regions displaying a possible association between the gene content and the specific neuroradiological anomalies:

- Smallest region of overlap (SRO) of 9,6 Mb spanning nucleotides 2,119,511 and 11,723,616, related to pontine hypoplasia;
- Critical region 1 (CR1) of 1,96 Mb spanning nucleotides 151,737 and 2,119,511, involved in the development of the CdCs brain structural abnormalities;
- Critical region 2 (CR2) of 2,4 Mb spanning nucleotides 11,723,616 and 14,153,620, related to vermian hypoplasia and ventricular anomalies;
- Critical region 3 (CR3) of 3,9 Mb spanning nucleotides 14,153,620 and 18,149,415, correlated to polymicrogyria.

4. Discussion

In the present study 14 patients, with different breakpoints of deletion of the short arm of chromosome 5, were evaluated from a clinical, neuroradiological and genetic point of view, using standard assessment criteria (clinical evaluation, neuroradiological investigation by brain MRI, genetic analysis by CGH-array). The aim was to investigate the presence of brain abnormalities detectable by nuclear magnetic resonance imaging and to establish a possible correlation with the size, position and gene content of the deletion.

Our series represent, to date, the largest cohort of patients with CdCS studied with MRI; moreover, it is the only cohort of patients in which a genotype-phenotype correlation focused on neuroradiological aspects has been proposed while, in the previous literature, critical regions have been identified related to other clinical features (e.g. characteristic cry or language delay) [23–30]. On the

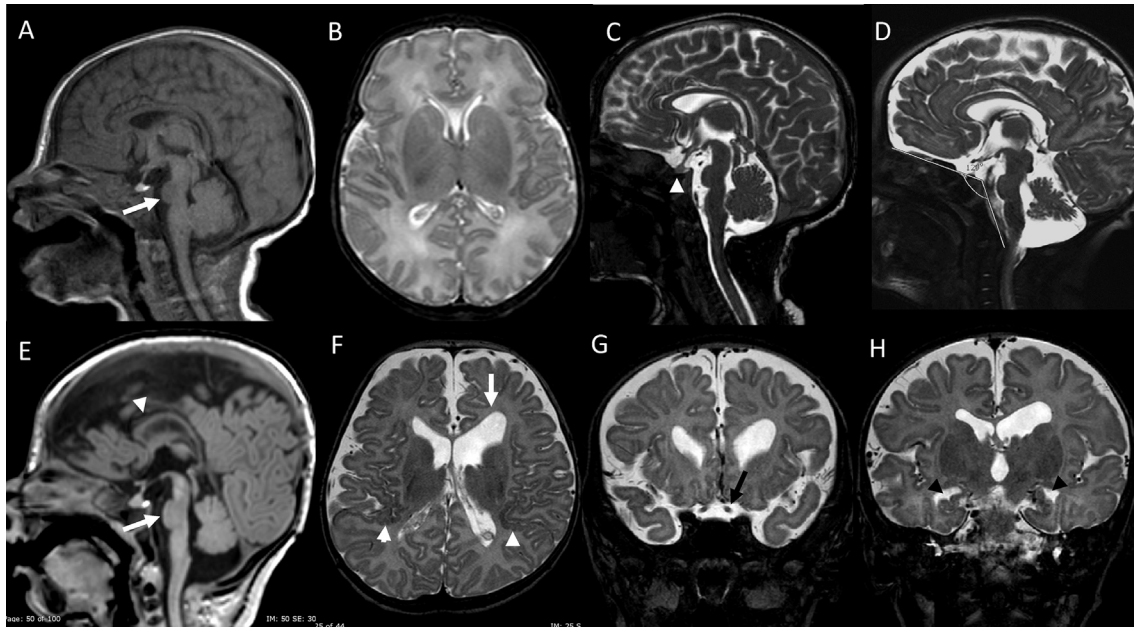


Fig. 2. Brain MRI findings. A, B, C) Patient #3: 5 days old with deletion of 11.6 Mb of the p15.33p15.2 region in the chromosome 5; sagittal T1 weighted image (A) shows pontine hypoplasia (white arrow); axial T2 weighted image (B) shows normal brain findings, with regular ventricular morphology and size; sagittal T2 weighted image (C) shows the widening of cavum sellae (white arrowhead). D) Patient #4: 53 days old with deletion of 12 Mb of the p15.33p15.2 region. The sagittal T2 image (D) shows platybasia with skull base angle of 129° (normal reference for children 114° ± 10°). E, F, G, H) Patient #2: 3 months old with deletion of 30.5 Mb of the p15.33p15.3 region in the chromosome 5. Sagittal T1 weighted image (E) shows pontine hypoplasia (white arrow) and thin corpus callosum (white arrowhead). Axial T2 weighted image (F) shows dysmorphic and enlarged ventricular system (white arrow) and bilateral perisylvian polymicrogyria (white arrowhead). Coronal T2 weighted images show (G) the optic nerve hypoplasia (black arrow) and (H) the hippocampus malrotation (black arrowhead).

Table 3
Genomic findings of the study cohort.

Patient	Deleted region	Proximal Breakpoint (hg19)	Distal Breakpoint (hg19)	Deletion size	Terminal/Interstitial	Inheritance	Additional CNVs (size)
1	5p15.33p15.2	151,737	12,699,724	12,5 Mb	T	De novo	no
2	5p15.33-p13.3	151,737	30,601,184	30, 5 Mb	T	De novo	no
3	5p15.33-p15.2	151,737	11,723,616	11,6 Mb	T	De novo	no
4	5p15.33p15.2	2,119,511	14,153,620	12 Mb	I	De novo	no
5	5p13.2	151,737	34,043,636	33,8 Mb	T	t(5;10)pat	arr[hg19] 10q25.3q26.3 (117059747_135404523)x3 (18,3 Mb)
6	5p15.2p14.1	13,779,728	26,594,000	12,8 Mb	I	De novo	no
7	5p15.33p15.1	2,119,511	18,149,415	16 Mb	I	De novo	arr[hg19] 10p13(12245205_12447468)x3 unk (202 Kb); arr[hg19] 6q22.31 (120195680_120308440)x1 unk (112 Kb)
8	5p15.33p15.2	151,737	11,723,616	11,6 Mb	T	De novo	arr[hg19] 6q15q16.1 (92723771_93609085)x3 unk (885Kb); arr[hg19] 19q13.2(41052830_41223762)x3 unk (171 Kb)
9	5p15.33p14	151,737	21,451,716	25,1 Mb	T	De novo	no
10	5p15.33p13.3	151,737	32,991,435	32,8 Mb	T	De novo	no
11	5p15.33p15.2	151,737	11,723,616	11,6 Mb	T	Unknown	arr[hg19] 15q26.2q26.3 (97257751_102531392)x3 unk (5,2 Mb)
12	5p15.33p15.2 ^a	151,737	14,153,620	14 Mb	T	Unknown	no
13	5p15.33p14.1	151,737	28,542,840	28,4 Mb	T	De novo	no
14	5p15.33p15.1	151,737	16,057,707	15,9 Mb	T	Unknown	no

^a Mosaic in 60% of cells.

other hand, the described cases in which neuroradiological characteristics are highlighted, are quite rare and no genotype-phenotype correlation has been proposed. Moreover, in the previously described cases (collected in the 1990s) [6,7] and in more recent case reports [7–19], the deletion of the short arm of chromosome 5 was identified mainly by classical cytogenetic analysis or, in one case, by FISH.

Data emerging from our analysis allowed us to expand and to specify the neuroradiological phenotype of CdCS, confirming the

presence, in the enrolled subjects, of the anomalies already described (hypoplasia of the brainstem and in particular of the pons, hypoplasia of the cerebellar vermis, increase of the basal angle and widening of the cavum sellae, dysmorphism or agenesis of the corpus callosum, dysmorphisms of the ventricles [38], and alterations of the white matter) [6–19]. Our data identified other features, such as polymicrogyria [reported only by Dmetrichuk et al., 20] and hypoplasia of the optical nerves, which has never been reported. Interestingly, there is a probable connection between the

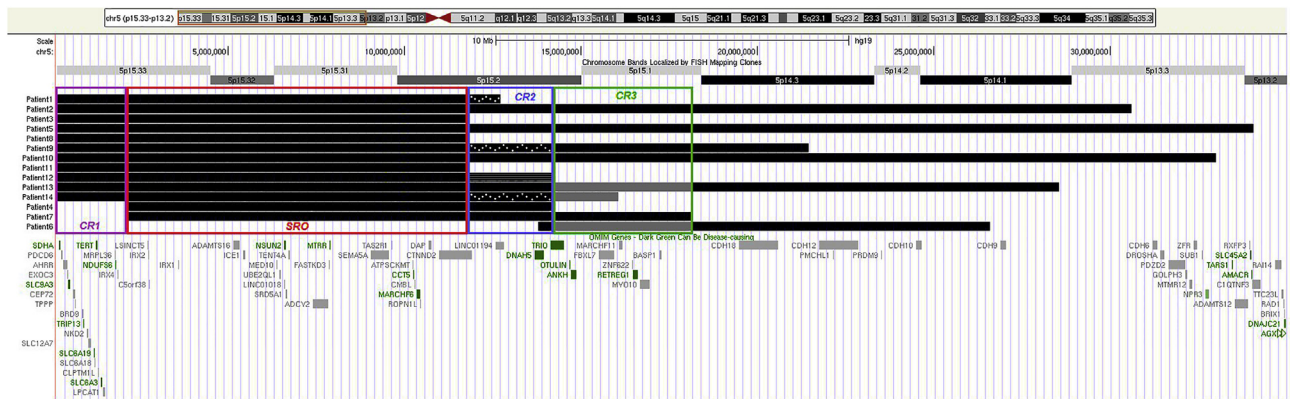


Fig. 3. Size and position of 5p deletions in our cohort and genotype and neuroradiologic findings correlation: SRO (Smallest region of overlap) of 9.6 Mb spanning nucleotides 2,119,511 and 11,723,616, related to pontine hypoplasia; CR1 (Critical region 1) of 1.96 Mb spanning nucleotides 151,737 and 2,119,511, probably contribute to development of the CdCs brain structural abnormalities; CR2 (Critical region 2) of 2.4 Mb spanning nucleotides 11,723,616 and 14,153,620, related to vermian hypoplasia and ventricular anomalies. Filled-in black bar represent patients with the presence of vermian hypoplasia and ventricular anomalies; black bar with white cross represent patients with only ventricular anomalies; black bar with grey lines represent patient with only vermian hypoplasia; CR3 (Critical region 3) of 3.9 Mb spanning nucleotides 14,153,620 and 18,149,415, correlated to polymicrogyria. Filled-in black bar represent patients with polymicrogyria; filled-in grey bar represent patients without polymicrogyria.

skull base anomalies depicted and the brainstem and cerebellar anomalies. The clivus and the cavum sellae are embryologically connected to the brainstem and cerebellar malformations, as the notochord is responsible for the development of the CNS and also of the axial skeleton [39–41]. Additionally, Kessel *et al.* [42] pointed out a tight developmental relationship between the hindbrain-spinal cord, the basisphenoid part of the axial skeleton and the glossopharyngeal–vagal ganglia that innervate the human larynx, suggesting a link between the brain and skull base anomalies and the characteristic cat-like cry typical of the Cri-du-Chat Syndrome.

By the comparison in size and location of the 5p deletions of our 14 patients (Fig. 3), it was possible to identify a SRO, shared by all cases showing pontine hypoplasia, with the exception of Patient #6.

Patient #6 displayed an interstitial deletion of 12.8 Mb, not included in the SRO, and showed microcephaly, hypotonia, psychomotor and language delay and health problems related to Cri-du-Chat Syndrome. His neuroradiological findings included hypoplasia and rotation of the cerebellar vermis, dysmorphic aspect of the ventricles and of corpus callosum. The absence of pontine hypoplasia suggests that the SRO gene content may contribute to pathogenesis of this abnormality.

Patient #5 and Patient #11 show large CNVs involving other chromosomes: a 18.3 Mb duplication of chromosome 10q and a 5.2 Mb duplication of chromosome 15q. In these regions map a very large number of genes, among them 22 OMIM Morbid genes on chromosome 10 and 7 on chromosome 15. Since genes involved in brain development and function are wide spread on the whole genome, some of them probably impact also on our findings, making the correlation with the 5p deletion features in these patients a challenge, while the small CNVs identified in Patient #7 and Patient #8 probably do not affect the clinical manifestations.

Several OMIM genes map in the SRO. Among them, the *IRX1* (OMIM*606197) and the *IRX2* (OMIM *606198) genes belong to the same family (*Iroquois Homeobox*) of the *IRX4* gene, which is situated distally and not included in the SRO. The *IRX1* gene is highly expressed in the diencephalon; Bosse *et al.*, 1997 showed that the group of the *IRX* genes is involved in several embryogenic processes, in particular in ventral-dorsal and antero-posterior patterning of specific regions of the CNS and in the regionalization of the auricular vesicle, branchial epithelium and cerebellum [43].

The *SEMA5A* gene (OMIM*609297) codes for a membrane protein that regulates axonal guidance and neuronal migration during

neural development [44]. Studies on the mouse and in particular on the expression pattern of *Sema5a* during brain development led to hypothesize a role of this gene in neuronal migration. Its haploinsufficiency could therefore cause development issues, intellectual disability and microcephaly observed in Cri du Chat individuals. Knockout mice for *Sema5a* have an increased number of excitatory synapses and, in behavioral studies, show an altered pattern of social interaction and, in particular, one reduction of interactions with other mice compared to control subjects [45,46]. Since alterations in the balance between excitatory and inhibitory synapses have been associated with neurobehavioral disorders such as autism [47], these data are consistent with the increase in the incidence of autism in hemizygous subjects for *SEMA5A*. The deletion of this gene is described in association with cerebral abnormalities, autism and ID [45,47,48].

The *CTNND2* gene (OMIM*604275) encodes for an adhesion protein with cell motility control function; it is expressed early in neurons during the development of the nervous system and it's thought to have a role in regulating neuronal migration. It could be implied in neuronal migration defects, such as those identified in our series. In the definition of genotype-phenotype correlations in patients with deletions of the short arm of chromosome 5, it was observed that subjects carrying deletions including *CTNND2* have more severe cognitive impairment [49], while studies in mice [50,51] indicate a possible relevance of *CTNND2* in maintaining the stability of dendritic structures. Further studies [52] seem to suggest a role of *CTNND2* in cerebellar Purkinje cell morphology.

In addition to the SRO, we pointed out other three possible critical regions (CR), correlated to pontine hypoplasia, polymicrogyria, vermian hypoplasia and ventricles abnormalities (Fig. 3).

In CR1 map at least 20 OMIM genes. Any of these show a direct association with brain structural abnormalities. Among them, the *IRX4* gene (OMIM*606199) shows involvement in several embryonic developmental processes, particularly of the specific region of central nervous system in mice [42].

Anyway, *SLC6A3*, *SLC6A19* and *SLC6A18* genes belong to the solute carrier 6 (SLC6) family. These genes' family encode neurotransmitter transporters, thus an altered expression could be associated with an altered neurotransmission and could contribute to the neurologic function [53].

TERT is commonly deleted in CdCs, but its direct role is unclear, as well as those of *CEP72* gene. *CEP72* is involved in regulation of

centrosomal proteins and mutations of this gene have been described to be associated with neurodevelopmental disorders [54]. Together, *CEP72*, *MRPL36*, *NDUFS6* and *TPPP* have been associated to hyperactivity and impulsiveness. *TPPP* gene and *SLC6A3* gene are described to mutually interact leading changes of pattern in neuronal activity in CdCs [55].

At present, the specific contribution given by this region to the brain structural abnormalities is unclear and additional research are needed to confirm the potential role of this region to the development of the CdCs brain structural abnormalities.

CR2 involves two genes: the 5' side of *TRIO* and the *DNAH5*. The *TRIO* gene (OMIM*601893) is highly expressed in the developing brain and it has been reported as a possible causative gene for intellectual disability and microcephaly. The index cases, originally described by Pengelly *et al.*, 2016, had mild cognitive impairment, microcephaly and minor facial abnormalities, in association with behavioral problems, such as autistic traits, hyperactivity and aggressiveness [56]. Anyway, CR2 region harbours just the exon 1-intron 1 of the *TRIO* gene. The 5' side of the gene lies within the spectrin repeats, while Trio-mediated Rac1 activation, the highly conserved Dbl homology–Pleckstrin homology (DH–PH) domains, is not included in this region. Mutations of the spectrin repeats do not seem to involve the Trio-mediated Rac1 activation, and the Trio function is not reported to be affected [56].

The *DNAH5* gene (OMIM*603335) encodes for the heavy chain of the assonemic dinein 5 and is one of the genes associated with Primary Ciliary Dyskinesia (OMIM #608644). The recessive status of *DNAH5* is described, in the mouse model, to be related to the onset of triventricular hydrocephalus by alteration of the ependymal flow. The high incidence of hydrocephalus in patients with ciliary defects demonstrates a possible role of this mechanism in humans [57]. The presence of widened and dysmorphic ventricles in patients #2, #9, #10 and #14, all showing the deletion of this gene could be related with this condition.

Haploinsufficiency of *DNAH5* could play a role in the genesis of vermian hypoplasia since its formation implies the involvement of genes associated to the ciliary functions [58]. Impaired cilia functions are known to disrupt neural circuitry and are also described in association with vermian hypoplasia as well as in other defects of brain development and neuronal migration [59].

CR3, correlated to polymicrogyria, encompasses *MYO10*, *BASP1* and the highly conserved domain of *TRIO*.

Cellular studies of the function of *TRIO* gene on rat neurons have demonstrated the effect of suppressing gene expression on dendritic structure formation and synapse development [60] and studies on mice with neural specific knock-out of *Trio*, showed that this gene may be a key signal module for the orchestrated regulation of neuronal migration and morphogenesis during cerebellar development [61]. Recently, a family with a novel *TRIO* gene mutation associated with the phenotype of cerebellar ataxia has been described [62].

The *MYO10* gene (OMIM*601481) encodes for myosin 10, an atypical member of the myosin family located at the end of the filopods, which is an important regulator of the cytoskeleton and affects cell motility and adhesion, although its effects *in vivo* are still largely unknown. Cellular studies have shown that several isoforms of myosin 10 are involved in radial migration of cortical neurons during the embryogenesis of the cerebral cortex [63] and that the knock-down of *MYO10* in neuronal cell lines causes a deficit in motility, cell orientation and matrix adhesion capacity [64]. Moreover, the suppression of the *MYO10* could cause an alteration of the expression of N-cadherin by damaging the ability of neurons to adhere to radial glial fibers in the development of the cerebral cortex [65].

It is also important to mention the *BASP1* gene (OMIM*605940), which encodes for a presynaptic membrane protein that acts on axonal growth, neuronal regeneration and synaptic plasticity

[66–68] and might play a role in the morphogenesis and development of brain structures.

Polymicrogyria have been described as a result of abnormal late cortical organization and associated with abnormal neuronal migration [69], the haploinsufficiency of the aforementioned genes have already be described in the genesis of this malformations.

5. Conclusions

Taking into account the limits due to the low number of patients examined, we can nonetheless speculate the existence of the smallest region of overlap in 5p15.33-15.2, which extends from the nucleotides 2,119,511 to 11,723,616 and is associated with the characteristic neuroradiological findings of brainstem, and in particular the pontine hypoplasia.

Although less evident, other possible genotype-phenotype correlations can be made with regard to ventricular anomalies, vermian hypoplasia and polymicrogyria.

The study of the gene content of these critical regions has pinpointed a few genes (such as *IRX4*, *SEMA5A*, *CTNND2*, *IRX1* and *IRX2*, *DNAH5*, *MYO10*, *TRIO* and *BASP1*) which could possibly play a role in the morphogenesis of specific cerebral structures. Microdeletions can act through different mechanisms: unmasking a recessive mutation, - a dosage sensitive gene may have a major effect, - a number of underexpressed dosage sensitive genes may show a cumulative effect.

Some of the genes included in the SRO, such as *SEMA5A* and *CTNND2*, are already classified as dosage sensitive, leading to haploinsufficiency, as well as *TERT* in CR1, while *SLC6A3*, in CR1, is a conditionally haploinsufficient gene acting together with others factors [70].

Overall, although some genes could play a primary role in the neuroradiological phenotype, the cumulative effect of dosage sensitive genes has a major impact on phenotype.

More data are however necessary to expand and confirm the genotype-phenotype correlations, in particular with the collection of more cases in which deletion size and position are identified by means of CMA analysis and the brain phenotype is investigated systematically by MRI scan with particular focus on the characteristic anomalies reported in CdCS patients. Identification of “outlier” patients, presenting less common features both in the genotype (i.e. interstitial deletions mapping more proximally and not including the critical regions correlated to specific MRI findings) and in the brain phenotype (i.e. patients presenting unreported anomalies or not presenting the more common ones) is obviously essential, but difficult when working on rare diseases. Thus, despite recent advances, our understanding of these heterogeneous neuroradiological malformations related to 5p deletions remains a challenge. It makes difficult to give an accurate genetic and prognostic counseling, and to provide the most appropriate management.

Further multicentric studies examining more wide case series will be necessary to deepen the genotype-brain phenotype correlations.

Declaration of competing interest

The authors declare that there are no conflicts of interests regarding financial, consultant, institutional or relationships.

Acknowledgments

The authors are grateful to the parents/guardians of the proband for their cooperation. This work has been promoted within the European Reference Network on Rare Congenital Malformations and Rare Intellectual Disability (ERN-ITHACA).

References

- [1] E. Niebuhr, The Cri du Chat syndrome: epidemiology, cytogenetics, and clinical features, *Hum. Genet.* 44 (3) (1978) 227–275, <https://doi.org/10.1007/BF00394291>.
- [2] E. Niebuhr, Cytologic observations in 35 individuals with a 5p- karyotype, *Hum. Genet.* 42 (2) (1978) 143–156, <https://doi.org/10.1007/BF00283634>.
- [3] P. Cerruti Mainardi, Cri du Chat syndrome, Orphanet J. Rare Dis. 1 (2006) 33, <https://doi.org/10.1186/1750-1172-1-33>. Published 2006 Sep. 5.
- [4] P.C. Mainardi, G. Pastore, C. Castronovo, et al., The natural history of Cri du Chat Syndrome. A report from the Italian Register, *Eur. J. Med. Genet.* 49 (5) (2006) 363–383, <https://doi.org/10.1016/j.ejmg.2005.12.004>.
- [5] P.C. Mainardi, C. Perfumo, A. Cali, et al., Clinical and molecular characterisation of 80 patients with 5p deletion: genotype-phenotype correlation, *J. Med. Genet.* 38 (3) (2001) 151–158, <https://doi.org/10.1136/jmg.38.3.151>.
- [6] G. De Michele, M. Presta, F. Di Salle, et al., Cerebellar vermiform hypoplasia in a case of cri-du-chat syndrome, *Acta Neurol.* 15 (2) (1993) 92–96.
- [7] J. Tamraz, M.O. Rethoré, J. Lejeune, et al., Morphométrie encéphalique en irm dans la maladie du chat. A propos de sept patients, avec revue de la littérature. Association pour la recherche sur la sclérose en plaques [Brain morphometry using MRI in Cri-du-Chat Syndrome. Report of seven cases with review of the literature], *Ann. Genet.* 36 (2) (1993) 75–87.
- [8] W.F. Arts, Y. Hofstee, G.F. Drejer, G.C. Beverstock, J.C. Oosterwijk, Cerebellar and brainstem hypoplasia in a child with a partial monosomy for the short arm of chromosome 5 and partial trisomy for the short arm of chromosome 10, *Neuropediatrics* 26 (1) (1995) 41–44, <https://doi.org/10.1055/s-2007-979718>.
- [9] C.P. Chen, C.C. Lee, T.Y. Chang, D.D. Town, W. Wang, Prenatal diagnosis of mosaic distal 5p deletion and review of the literature, *Prenat. Diagn.* 24 (1) (2004) 50–57, <https://doi.org/10.1002/pd.794>.
- [10] F. Vialard, R. Robyr, Y. Hillion, D. Molina Gomes, J. Selva, Y. Ville, Dandy-Walker syndrome and corpus callosum agenesis in 5p deletion, *Prenat. Diagn.* 25 (4) (2005) 311–313, <https://doi.org/10.1002/pd.1130>.
- [11] X.H. Teoh, T.Y. Tan, K.K. Chow, I.W. Lee, Prenatal diagnosis of cri-du-chat syndrome: importance of ultrasonographical markers, *Singap. Med. J.* 50 (5) (2009) e181–e184.
- [12] T. Ninchoji, J. Takanashi, Pontine hypoplasia in 5p-syndrome: a key MRI finding for a diagnosis, *Brain Dev.* 32 (7) (2010) 571–573, <https://doi.org/10.1016/j.braindev.2009.07.003>.
- [13] Z. Kato, N. Kondo, H. Kato, et al., Selective pontine hypoplasia: a possible common feature in 5p monosomy syndrome, *Brain Dev.* 33 (8) (2011) 702–703, <https://doi.org/10.1016/j.braindev.2010.11.004>.
- [14] C.P. Chen, M.C. Huang, Y.Y. Chen, et al., Cri-du-chat (5p-) syndrome presenting with cerebellar hypoplasia and hypospadias: prenatal diagnosis and aCGH characterization using uncultured amniocytes, *Gene* 524 (2) (2013) 407–411, <https://doi.org/10.1016/j.gene.2013.03.003>.
- [15] J.H. Hong, H.Y. Lee, M.K. Lim, et al., Brain stem hypoplasia associated with Cri-du-Chat syndrome, *Korean J. Radiol.* 14 (6) (2013) 960–962, <https://doi.org/10.3348/kjr.2013.14.6.960>.
- [16] T.A. Uzunhan, B. Sayınbatur, M. Çalışkan, A. Sahin, K. Aydın, A clue in the diagnosis of Cri-du-chat syndrome: pontine hypoplasia, *Ann. Indian Acad. Neurol.* 17 (2) (2014) 209–210, <https://doi.org/10.4103/0972-2327.132635>.
- [17] R. Nandhagopal, A.M. Udayakumar, Cri-du-chat syndrome, *Indian J. Med. Res.* 140 (4) (2014) 570–571.
- [18] D.G. Corrêa, N. Ventura, E.L. Gasparetto, Pontine hypoplasia in cri-du-chat syndrome: alterations in diffusion tensor imaging, *Childs Nerv. Syst.* 33 (8) (2017) 1241–1242, <https://doi.org/10.1007/s00381-017-3508-9>.
- [19] D. Kaymak, V. Alpay, H. Erenel, I. Adaletli, N. Comunoglu, R. Madazli, Prenatal diagnosis of 5p deletion syndrome with brain abnormalities by ultrasonography and fetal magnetic resonance imaging: a case report [published online ahead of print, 2019 sep 25], *Fetal Pediatr Pathol*, 2019, pp. 1–6, <https://doi.org/10.1080/15513815.2019.1669230>.
- [20] J.M. Dmetrichuk, D.A. Chiasson, J.Q. Lu, Neuronal inclusions and α -Synucleinopathy in a patient with 5p deletion syndrome, *J. Neurol. Sci.* 403 (2019) 56–58, <https://doi.org/10.1016/j.jns.2019.05.036>.
- [21] I. Kjaer, E. Niebuhr, Studies of the cranial base in 23 patients with cri-du-chat syndrome suggest a cranial developmental field involved in the condition, *Am. J. Med. Genet.* 82 (1) (1999) 6–14, [https://doi.org/10.1002/\(sici\)1096-8628\(19990101\)82:1<6::aid-ajmg2>3.0.co;2-#](https://doi.org/10.1002/(sici)1096-8628(19990101)82:1<6::aid-ajmg2>3.0.co;2-#).
- [22] M.E. Liverani, A. Spano, C. Danesino, et al., Children and adults affected by Cri du Chat syndrome: care's recommendations, *Pediatr. Rep.* 11 (1) (2019) 7839, <https://doi.org/10.4081/pr.2019.7839>. Published 2019 Feb 26.
- [23] J.M. Nguyen, K.J. Qualmann, R. Okashah, A. Reilly, M.F. Alexeyev, D.J. Campbell, 5p deletions: current knowledge and future directions, *Am. J. Med. Genet. C Semin. Med. Genet.* 169 (3) (2015) 224–238, <https://doi.org/10.1002/ajmg.c.31444>.
- [24] J. Overhauser, X. Huang, M. Gersh, et al., Molecular and phenotypic mapping of the short arm of chromosome 5: sublocalization of the critical region for the cri-du-chat syndrome, *Hum. Mol. Genet.* 3 (2) (1994) 247–252, <https://doi.org/10.1093/hmg/3.2.247>.
- [25] Q. Wu, E. Niebuhr, H. Yang, L. Hansen, Determination of the 'critical region' for cat-like cry of Cri-du-chat syndrome and analysis of candidate genes by quantitative PCR, *Eur. J. Hum. Genet.* 13 (4) (2005) 475–485, <https://doi.org/10.1038/sj.ejhg.5201345>.
- [26] X. Zhang, A. Snijders, R. Seagraves, et al., High-resolution mapping of genotype-phenotype relationships in cri du chat syndrome using array comparative genomic hybridization, *Am. J. Hum. Genet.* 76 (2) (2005) 312–326, <https://doi.org/10.1086/427762>.
- [27] T. Kondoh, O. Shimokawa, N. Harada, et al., Genotype-phenotype correlation of 5p-syndrome: pitfall of diagnosis, *J. Hum. Genet.* 50 (1) (2005) 26–29, <https://doi.org/10.1007/s10038-004-0213-9>.
- [28] A. Elmakky, D. Carli, L. Lugli, et al., A three-generation family with terminal microdeletion involving 5p15.33-32 due to a whole-arm 5;15 chromosomal translocation with a steady phenotype of atypical cri du chat syndrome, *Eur. J. Med. Genet.* 57 (4) (2014) 145–150, <https://doi.org/10.1016/j.ejmg.2014.02.005>.
- [29] L.D. Espirito Santo, L.M. Moreira, M. Riegel, Cri-du-Chat syndrome: clinical profile and chromosomal microarray analysis in six patients, *BioMed Res. Int.* 2016 (2016), <https://doi.org/10.1155/2016/5467083>, 5467083.
- [30] J.M. Nguyen, K.J. Qualmann, R. Okashah, A. Reilly, M.F. Alexeyev, D.J. Campbell, 5p deletions: current knowledge and future directions, *Am. J. Med. Genet. C Semin. Med. Genet.* 169 (3) (2015) 224–238, <https://doi.org/10.1002/ajmg.c.31444>.
- [31] C. Jandeaux, G. Kuchcinski, C. TERNYNCK, et al., Biometry of the cerebellar vermis and brain stem in children: MR imaging reference data from measurements in 718 children, *AJNR Am. J. Neuroradiol.* 40 (11) (2019) 1835–1841, <https://doi.org/10.3174/ajnr.A6257>.
- [32] R. Yang, R. Li, X. Liu, et al., Measurement of fetal mesencephalon and pons via ultrasonographic cross sectional imaging, *Fetal Pediatr. Pathol.* 37 (1) (2018) 38–48, <https://doi.org/10.1080/15513815.2017.1397069>.
- [33] S.Ö. Polat, F.Y. Öksüzler, M. Öksüzler, A.H. Yücel, The morphometric measurement of the brain stem in Turkish healthy subjects according to age and sex, *Folia Morphol. (Wars.)* 79 (1) (2020) 36–45, <https://doi.org/10.5603/FM.a2019.0085>.
- [34] C.E. Al-Haddad, M.G. Sebaaly, R.N. Tutunji, et al., Optic nerve measurement on MRI in the pediatric population: normative values and correlations, *AJNR Am. J. Neuroradiol.* 39 (2) (2018) 369–374, <https://doi.org/10.3174/ajnr.A5456>.
- [35] R.A. Koenigsberg, N. Vakili, T.A. Hong, et al., Evaluation of platybasia with MR imaging, *AJNR Am. J. Neuroradiol.* 26 (1) (2005) 89–92.
- [36] J. McGowan-Jordan, A. Simons, M. Schmid (Eds.), *ISCN 2016: an International System for Human Cytogenomic Nomenclature*, *Cytogenet Genome Res.* vol. 149, 2016, pp. 1–140.
- [37] R.J. Hastings, S. Cavani, F.D. Bricarelli, P.C. Patsalis, U. Kristofferson, ECA PWC Co-ordinators. Cytogenetic Guidelines and Quality Assurance: a common European framework for quality assessment for constitutional and acquired cytogenetic investigations, *Eur. J. Hum. Genet.* 15 (5) (2007) 525–527, <https://doi.org/10.1038/sj.ejhg.5201809>.
- [38] CL Scelsi, TA Rahim, JA Morris, GJ Kramer, BC Gilbert, SE Forseen, The lateral ventricles: A detailed review of anatomy, development, and anatomic variations, *AJNR Am. J. Neuroradiol.* 41 (4) (2020) 566–572, <https://doi.org/10.3174/ajnr.A6456>.
- [39] R. Balling, U. Helwig, J. Nadeau, A. Neubüser, W. Schmahl, K. Imai, Pax genes and skeletal development, *Ann. N. Y. Acad. Sci.* 785 (1996) 27–33, <https://doi.org/10.1111/j.1749-6632.1996.tb56240.x>.
- [40] I. Kjaer, The prenatal axial skeleton as marker of normal and pathological development of the human central nervous system, in: H.C. Lou, G. Greisen, J.F. Larsen (Eds.), *Brain Lesions of the Newborn*, Alfred Benzon Symposium 37, Munksgaard, Copenhagen, 1994, pp. 124–132.
- [41] I. Kjaer, A. Wagner, P. Madsen, S. Blichfeldt, K. Rasmussen, B. Russell, The sella turcica in children with lumbosacral myelomeningocele, *Eur. J. Orthod.* 20 (4) (1998) 443–448, <https://doi.org/10.1093/ejo/20.4.443>.
- [42] M. Kessel, Reversal of axonal pathways from rhombomere 3 correlates with extra Hox expression domains, *Neuron* 10 (3) (1993) 379–393, [https://doi.org/10.1016/0896-6273\(93\)90328-o](https://doi.org/10.1016/0896-6273(93)90328-o).
- [43] A. Bosse, A. Zülch, M.B. Becker, et al., Identification of the vertebrate Iroquois homeobox gene family with overlapping expression during early development of the nervous system, *Mech. Dev.* 69 (1–2) (1997) 169–181, [https://doi.org/10.1016/s0925-4773\(97\)00165-2](https://doi.org/10.1016/s0925-4773(97)00165-2).
- [44] R.H. Adams, H. Betz, A.W. Püschel, A novel class of murine semaphorins with homology to thrombospondin is differentially expressed during early embryogenesis, *Mech. Dev.* 57 (1) (1996) 33–45, [https://doi.org/10.1016/0925-4773\(96\)00525-4](https://doi.org/10.1016/0925-4773(96)00525-4).
- [45] A.D. Simmons, J. Overhauser, M. Lovett, Isolation of cDNAs from the Cri-du-chat critical region by direct screening of a chromosome 5-specific cDNA library, *Genome Res.* 7 (2) (1997) 118–127, <https://doi.org/10.1101/gr.7.2.118>.
- [46] Y. Duan, S.H. Wang, J. Song, et al., Semaphorin 5A inhibits synaptogenesis in early postnatal- and adult-born hippocampal dentate granule cells, *Elife* 3 (2014), <https://doi.org/10.7554/elife.04390>.
- [47] P. Penzes, M.E. Cahill, K.A. Jones, J.E. VanLeeuwen, K.M. Woolfrey, Dendritic spine pathology in neuropsychiatric disorders, *Nat. Neurosci.* 14 (3) (2011) 285–293, <https://doi.org/10.1038/nrn.2741>.
- [48] L.A. Weiss, D.E. Arking, Gene discovery project of Johns Hopkins & the autism consortium, Daly MJ, Chakravarti A. A genome-wide linkage and association scan reveals novel loci for autism, *Nature* 461 (7265) (2009) 802–808, <https://doi.org/10.1038/nature08490>.
- [49] M. Medina, R.C. Marinescu, J. Overhauser, K.S. Kosik, Hemizygoty of delta-catenin (CTNND2) is associated with severe mental retardation in cri-du-chat syndrome, *Genomics* 63 (2) (2000) 157–164, <https://doi.org/10.1006/geno.1999.6090>.

- [50] C. Matter, M. Pribadi, X. Liu, J.T. Trachtenberg, Delta-catenin is required for the maintenance of neural structure and function in mature cortex in vivo, *Neuron* 64 (3) (2009) 320–327, <https://doi.org/10.1016/j.neuron.2009.09.026>.
- [51] L. Yuan, E. Seong, J.L. Beuscher, J. Arikath, δ -Catenin regulates spine architecture via cadherin and PDZ-dependent interactions, *J. Biol. Chem.* 290 (17) (2015) 10947–10957, <https://doi.org/10.1074/jbc.M114.632679>.
- [52] A.F. van Rootselaar, A.J. Groffen, B. de Vries, et al., δ -Catenin (CTNND2) missense mutation in familial cortical myoclonic tremor and epilepsy, *Neurology* 89 (23) (2017) 2341–2350, <https://doi.org/10.1212/WNL.0000000000004709>.
- [53] L. Lin, S.W. Yee, R.B. Kim, K.M. Giacomini, SLC transporters as therapeutic targets: emerging opportunities, *Nat. Rev. Drug Discov.* 14 (8) (2015) 543–560, <https://doi.org/10.1038/nrd4626>.
- [54] A. Kodani, T.W. Yu, J.R. Johnson, et al., Centriolar satellites assemble centrosomal microcephaly proteins to recruit CDK2 and promote centriole duplication, *Elife* 4 (2015), <https://doi.org/10.7554/eLife.07519>.
- [55] T. Corrêa, B.C. Feltes, M. Riegel, Integrated analysis of the critical region 5p15.3-p15.2 associated with cri-du-chat syndrome, *Genet. Mol. Biol.* 42 (1 suppl 1) (2019) 186–196, <https://doi.org/10.1590/1678-4685-GMB-2018-0173>.
- [56] R.J. Pengelly, S. Greville-Heygate, S. Schmidt, et al., Mutations specific to the Rac-GEF domain of TRIO cause intellectual disability and microcephaly, *J. Med. Genet.* 53 (11) (2016) 735–742, <https://doi.org/10.1136/jmedgenet-2016-103942>.
- [57] I. Ibañez-Tallon, A. Pagenstecher, M. Fliegau, et al., Dysfunction of axonemal dynein heavy chain Mdnah5 inhibits ependymal flow and reveals a novel mechanism for hydrocephalus formation, *Hum. Mol. Genet.* 13 (18) (2004) 2133–2141, <https://doi.org/10.1093/hmg/ddh219>.
- [58] J.F. Reiter, M.R. Leroux, Genes and molecular pathways underpinning ciliopathies, *Nat. Rev. Mol. Cell Biol.* 18 (9) (2017) 533–547, <https://doi.org/10.1038/nrm.2017.60>.
- [59] J. Guo, H. Higginbotham, J. Li, et al., Developmental disruptions underlying brain abnormalities in ciliopathies, *Nat. Commun.* 6 (2015) 7857, <https://doi.org/10.1038/ncomms8857>.
- [60] W. Ba, Y. Yan, M.R. Reijnders, et al., TRIO loss of function is associated with mild intellectual disability and affects dendritic branching and synapse function, *Hum. Mol. Genet.* 25 (5) (2016) 892–902, <https://doi.org/10.1093/hmg/ddv618>.
- [61] Y.J. Peng, W.Q. He, J. Tang, et al., Trio is a key guanine nucleotide exchange factor coordinating regulation of the migration and morphogenesis of granule cells in the developing cerebellum, *J. Biol. Chem.* 285 (32) (2010) 24834–24844, <https://doi.org/10.1074/jbc.M109.096537>.
- [62] R. Hanna Al Shaikh, T. Caulfield, A.J. Strongosky, et al., TRIO gene segregation in a family with cerebellar ataxia, *Neurol. Neurochir. Pol.* 52 (6) (2018) 743–749, <https://doi.org/10.1016/j.pjnns.2018.09.006>.
- [63] X.D. Ju, Y. Guo, N.N. Wang, et al., Both Myosin-10 isoforms are required for radial neuronal migration in the developing cerebral cortex, *Cerebr. Cortex* 24 (5) (2014) 1259–1268, <https://doi.org/10.1093/cercor/bhs407>.
- [64] H. Yu, M. Lai, Y. Guo, et al., Myo10 is required for neurogenic cell adhesion and migration, *In Vitro Cell. Dev. Biol. Anim.* 51 (4) (2015) 400–407, <https://doi.org/10.1007/s11626-014-9845-z>.
- [65] M. Lai, Y. Guo, J. Ma, et al., Myosin X regulates neuronal radial migration through interacting with N-cadherin, *Front. Cell. Neurosci.* 9 (2015) 326, <https://doi.org/10.3389/fncel.2015.00326>.
- [66] M.I. Mosevitsky, Nerve ending "signal" proteins GAP-43, MARCKS, and BASP1, *Int. Rev. Cytol.* 245 (2005) 245–325, [https://doi.org/10.1016/S0074-7696\(05\)45007-X](https://doi.org/10.1016/S0074-7696(05)45007-X).
- [67] E. Kropotova, B. Klementiev, M. Mosevitsky, BASP1 and its N-end fragments (BNEMFs) dynamics in rat brain during development, *Neurochem. Res.* 38 (6) (2013) 1278–1284, <https://doi.org/10.1007/s11064-013-1035-y>.
- [68] I. Korshunova, P. Caroni, K. Kolkova, V. Berezin, E. Bock, P.S. Walmod, Characterization of BASP1-mediated neurite outgrowth, *J. Neurosci. Res.* 86 (10) (2008) 2201–2213, <https://doi.org/10.1002/jnr.21678>.
- [69] R. Guerrini, E. Parrini, Neuronal migration disorders, *Neurobiol. Dis.* 38 (2) (2010) 154–166, <https://doi.org/10.1016/j.nbd.2009.02.008>.
- [70] J.M. Nguyen, K.J. Qualmann, R. Okashah, A. Reilly, M.F. Alexeyev, D.J. Campbell, 5p deletions: current knowledge and future directions, *Am. J. Med. Genet. C Semin. Med. Genet.* 169 (3) (2015) 224–238, <https://doi.org/10.1002/ajmg.c.31444>.